

Hydrogen-assisted cold cracking in welded joints of press-hardened 22MnB5

Olaf Schwedler¹  · Niels Holtschke¹ · Sven Jüttner¹

Received: 22 February 2016 / Accepted: 10 June 2016 / Published online: 22 June 2016
© International Institute of Welding 2016

Abstract Over the last decade, press hardening has become all pervasive for automotive body-in-white design. Press-hardened boron micro-alloyed steels are widely used in modern body structure for high safety standard and lightweight achievement. Considering the welding of press-hardened components, some special considerations have to be taken into account compared to conventional deep-drawing steel grades. The mechanical properties of the welded joints are influenced by the hydrogen content in the base metal as well as the weld metal. Hydrogen absorption may result from the press-hardening process, as well as the welding process. Due to the martensitic microstructure and the high strength level, a critical hydrogen content may cause hydrogen embrittlement or hydrogen-assisted cold cracking (HACC). This paper focuses on the determination of the diffusible hydrogen content in the base metal after the press-hardening process, as well as in gas metal arc (GMA) welded joints of 22MnB5. Hydrogen source during press hardening is the humidity at the austenitizing temperature in the furnace atmosphere. During welding, for this study hydrogen was deliberately introduced by hydrogenous fluids on the sheet surface. The diffusible hydrogen content in the base metal and the weld metal was quantified by thermal desorption mass spectroscopy (TDMS) technique. The influence of the diffusible hydrogen on the mechanical properties of the welds was determined by four-

point-bend testing. The time to fracture was identified using acoustic emission technique.

Keywords (IIW Thesaurus) GMA welding · Welded joints · High strength steels · Heat affected zone · Hydrogen · Cold cracking

1 Introduction

To reduce fuel consumption and CO₂ emissions by reducing vehicle weight, efforts to implement a lightweight concept in automotive industry were first made in the 1990s [1]. This ambition for weight reduction has been pursued consistently in the last few decades. This trend led to the use of ultrahigh-strength steel (UHSS) grades in automobile bodies, which results in the ability to reduce sheet thickness at the same or higher strength compared to conventional steels [2]. A method for the manufacturing of car body parts made of high-strength steels is a manufacturing process known as hot stamping or press hardening. The press-hardening process combines the advantages of spring-back-free hot-formed metal sheets with a hardening heat treatment. This generates car body parts with maximum strength (up to 1600 MPa) which adapt the highly complex shapes given by a modern automobile design. The material most widely used for press hardening is a boron alloyed steel, known as 22MnB5 (material number 1.5528). Due to its high strength, it is primarily used in safety-relevant components of the car body, i.e., A- and B-pillar reinforcements, and side impact protection such as longitudinal and cross-members.

The advantages of the use of press-hardened steel are offset by concerns regarding the occurrence of hydrogen embrittlement or hydrogen-assisted cold cracking (HACC) in the base metal or welded structures. This is a delayed and therefore unpredictable occurring material degradation. The conditions

Recommended for publication by Commission II - Arc Welding and Filler Metals

✉ Olaf Schwedler
olaf.schwedler@ovgu.de

¹ Institute of Materials and Joining Technology, Otto-von-Guericke University Magdeburg, Magdeburg, Germany

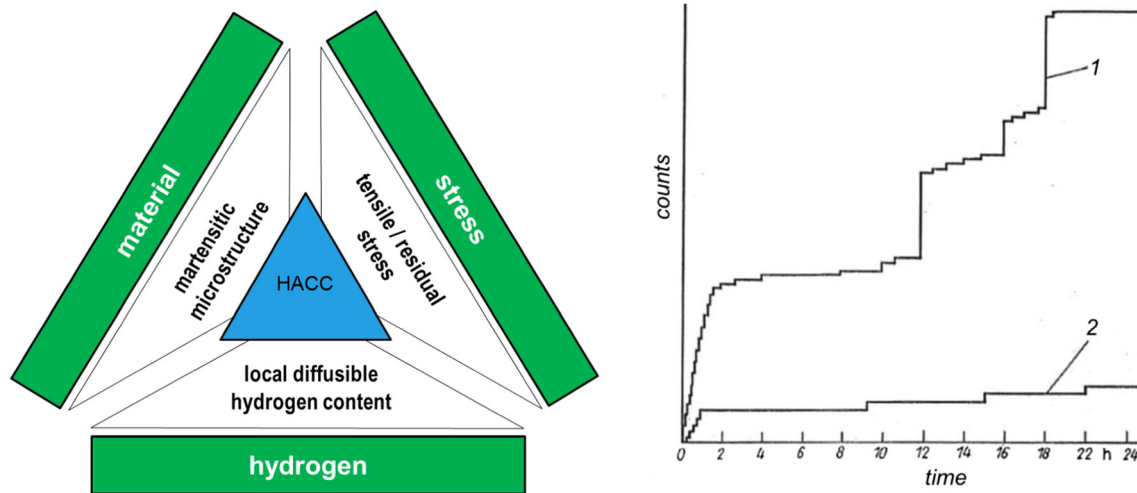


Fig. 1 Conditions for hydrogen-assisted cold cracking (HACC) (left). Acoustic emission diagram showing the difference in cumulative acoustic energy curves for a sample with cracking (1) and without cracking (2) [14] (right)

for HACC are illustrated in Fig. 1—left. HACC results from an interaction of diffusible hydrogen, a hardened martensitic microstructure, and stresses, i.e., external and internal tensile stresses [3]. The introduction of diffusible hydrogen can occur during the press-hardening process, especially during the austenitization of 22MnB5 at temperatures between 900 and 950 °C [4]. An aluminum-silicon coating (+AS150, i.e., 150 g/m²) counteracts a decarburization and scaling of the steel substrate during the furnace process. According to [5], the furnace temperature, the dwell time, and in particular the dew point of the furnace atmosphere are crucial for a pickup of hydrogen into the 22MnB5 material during the press-hardening process. In series production, the dew point is set usually between 3 and 12 °C.

The hydrogen absorption during press hardening is governed by the high affinity of the aluminum in the Al-Si coating of the steel sheets. Water molecules in the furnace atmosphere dissociate in two hydrogen ions and one oxygen ion. Part of the hydrogen ions recombines to form molecular hydrogen and moves back into the ambient atmosphere. Another part of the hydrogen ions is attracted by the free electrons of the metal surface and is absorbed into the metallic matrix. The oxygen combines at the surface of the aluminum to the corresponding metal oxide Al₂O₃.

In addition to the hydrogen pickup in the furnace during the press-hardening process, hydrogen can also be introduced during welding processes.

During arc welding, very high temperatures occur, which cause molecular hydrogen to dissociate in the arc. This hydrogen is then introduced into the liquid weld pool [3]. Possible sources of hydrogen that may be present during arc welding are given in Table 1.

For the welding of press-hardened components, resistance spot welding (RSW) and gas metal arc welding (GMAW) are exclusively used [7]. During welding component deviations, i.e., geometric variations and deformations as well as positional deviations, are decisive for the stress state, especially within the location of the weld [6]. Geometric changes in the weld cross section and microstructural changes in both the weld metal and the heat-affected zone contribute to the presence of a multiaxial stress state in the welds. This constitutes a further condition for HACC.

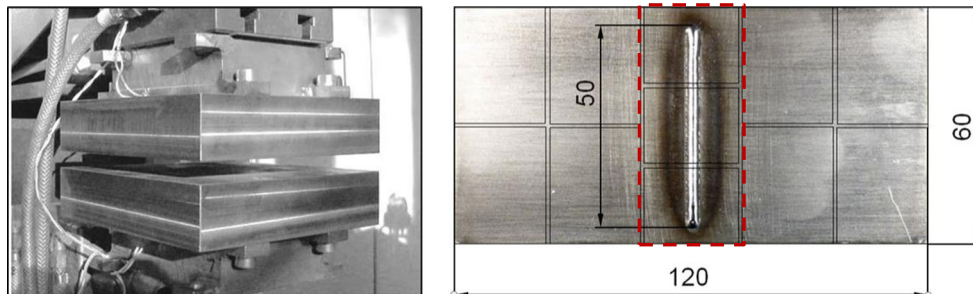
There are a large number of cold-cracking tests to verify the susceptibility of welds. A clear overview is given in [8]. However, all these tests are for a sheet thickness ≥ 6 mm. Their transferability for welding on thin sheets is therefore limited. In [9] different cold-cracking test methods have been reviewed for their suitability and possible application for high-strength steel sheets. One way of testing for HACC susceptibility is the four-point-bend test. Its suitability has been extensively proven for welds on 22MnB5 [10–12]. Extensive knowledge in testing press-hardened 22MnB5+AS150 for HACC using the four-point-bend test is described in [5]. Influences on the cold-cracking behavior of the un-welded

Table 1 Hydrogen sources in arc welding

Manufacturing effects	Environmental effects	Technological effects
<ul style="list-style-type: none"> •Metallurgical hydrogen (steel production) •Drawing grease on filler metal •Hydrogen in shielding gas 	<ul style="list-style-type: none"> •Surface contamination (preservative oil, paint residues, etc.) •Atmospheric inclusions (crystal water in electrode covering, welding powder, condensation water) •Coating components, i.e., Al(OH)₃ on Al parts 	<ul style="list-style-type: none"> •Torch positioning (tilt angle, setting angle, stick-out) •Wrong shielding gas settings •Moisture on leakage

Table 2 Chemical composition of 22MnB5

C	Mn	Si	P	Al	Ti	Cr	B	Mo	Cu	Ni
0.22	1.15	0.23	0.018	0.034	0.035	0.18	0.0027	<0.005	0.017	0.013

Fig. 2 Sheet dies $F_{\max} = 6.5$ kN (left). Four-point-bend test sample with a GMAW bead-on-plate, rectangles characterize separated samples for diffusible hydrogen determination (right)

material were the hydrogen content in the press-hardened sheets resulting from different dew points in the roller hearth furnace and different cooling rates. A multiaxial stress state occurred due to shear-cut edges which were prepared with various cutting gaps (sheared edges vs. machined edges).

The result of cold-cracking tests usually includes only a qualitative statement with the occurrence of cracks or no cracks. The test sample are subjected to stress conditions, which may be self- or externally stressed, and which is constant over a defined period of time. After the test, quality assessment is made by visual inspection and microsection. In order to get a quantitative results, e.g., about the time to the occurrence of cracks, non-destructive testing (NDT) by acoustic emission technique has proven to be advantageous. Sound waves caused by crack events are converted into electrical signals and are thus available for evaluation. HACC can be well detected with the acoustic emission technique. [13, 14] As Fig. 1 (right) illustrates, there are clear differences within the cumulative curves of the acoustic energy plotted over time. Curve 1 is characterized by a strong increase in cumulative energy, indicating the occurrence of cracking, while curve 2 is not subjected to cracking.

2 Experimental

2.1 Materials and sample preparation

For the investigations, boron manganese steel 22MnB5+AS150 sheets with a thickness of 1.5 mm were used. The chemical composition of the material is given in Table 2.

The press hardening of the material was performed on a laboratory press hardening. The heating and austenitization of the sheets was done in a laboratory oven at 930 °C for a period of 6 min. To protect the steel substrate against scaling during the furnace process, the sheet surface is covered with an aluminum-silicon coating (150 g/m²). After austenitization,

the sheets were put manually into the cooling die. A sufficiently high cooling rate of about 85 K/s was achieved by using sheet dies (Fig. 2—left). After the press hardening, the mechanical properties of the now fully martensitic material are different as compared to the initial ferritic-pearlitic condition (Table 3).

For the four-point-bend test, flat samples were used with the final contours as shown in Fig. 2—right. The four-point-bend test was used to test for cold cracking of welded steel sheets with a thickness ≤ 3.0 mm. During bending, the sample is supported in the bending device by two outer bearings, and it is loaded between the inner bearings with a force symmetrically to the center of the sample. The required bending stress is set via the path f of the punch (Fig. 3). Due to the fact that the test load (i.e., the bending stress) is applied in a defined and quantifiable way, it is an externally loaded test.

For GMA welding, the cold metal transfer (CMT) process, a modified short-arc welding process was used. All welds were done as a bead-on-plate weld (50 mm in length) in the center of the test sample. The used welding parameters are shown in Table 4.

The chemical composition of the filler metal is given in Table 5. Due to the lower carbon content of the filler metal, a faster transformation of austenite (FCC) into the ferritic phase (BCC) takes place during cooling after welding. Austenite exhibits low hydrogen diffusivity and high hydrogen solubility, whereas ferrite has high hydrogen diffusivity and low hydrogen solubility. These differences in hydrogen transportation behavior lead to a hydrogen trapping which principally bears potential with regard to HACC.

Table 3 Mechanical properties of 22MnB5

	Tensile strength R_m (MPa)	Yield strength $R_{p0.2}$ (MPa)	Elongation A_{50} (%)
Initial state	602	471	15.1
After press hardening	1466	1007	7.0

Fig. 3 Four-point-bend test device with gauge to set the travel distance f (left). Travel distance f -extreme fiber stress σ curve (right)

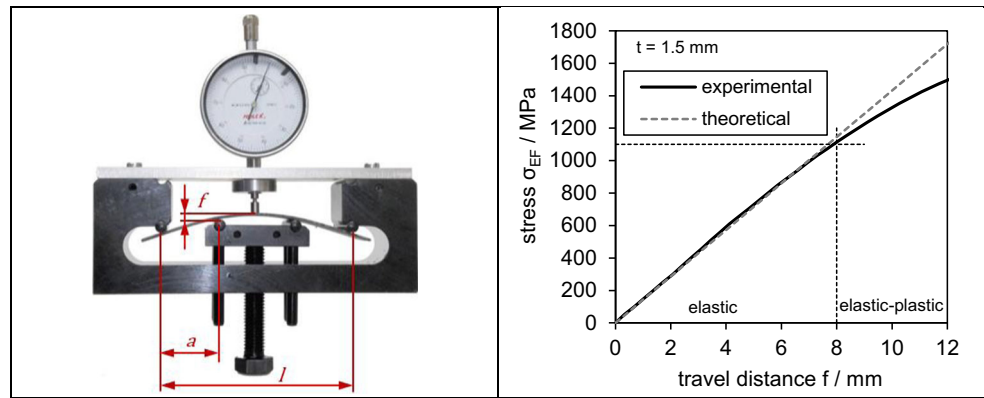
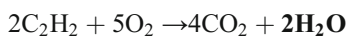


Table 4 Welding parameters for gas metal arc welding (CMT process) of 22MnB5+AS150

Shielding gas	18 % CO ₂ , Bal. Ar	Filler metal	G3Si1 (Ø 1.0 mm)
Welding speed (cm/min)	70	Wire speed (m/min)	2.5
Current (A)	95/76	Voltage (V)	20/15

2.2 Introduction of hydrogen

For this study, hydrogen was introduced into the 22MnB5 samples in two ways. The first way was a hydrogen pickup during austenitization in the press-hardening process. This was done by exposing the material in a retort furnace to an atmosphere with a constant dew point. The actual dew point was measured in situ with a dew point hygrometer. A dew point D_p of 10 °C and a much higher dew point of about 45 °C were investigated. The higher dew point was achieved by passing combustion gas, formed during the combustion of acetylene, into the retort. Carbon dioxide and water formed by the combustion of an acetylene-oxygen mixture, shown in the following equation:



Another way of hydrogen adsorption was studied in the presence of hydrogen-containing media on the surface of the sheets during GMA welding. For this purpose, the sheet surfaces were wetted with water or preservative oil before welding. While water on the surface is imitating condensation or burner leaks, preservative oil is used in industrial practice

for the protection of the components during transport and storage.

To determine the hydrogen-dependent cold-cracking behavior, five different groups of samples with different hydrogen content (Table 6) were prepared with the described ways of hydrogen introduction in the furnace or during the welding process. For differentiation of the hydrogen content introduced in both ways, some samples were additionally soaked after the press-hardening process at a temperature of 180 °C for a period of 20 min. During soaking the diffusible hydrogen, which was adsorbed during the press-hardening process, is removed from the material prior to GMA welding.

2.3 Quantification of hydrogen

Quantification of diffusible hydrogen was done by hot gas extraction with a Galileo G8. For this purpose, the middle of the samples with the GMA bead-on-plate weld was mechanically cut into three pieces (Fig. 2—right). This was done to get information of the distribution of diffusible hydrogen along the weld bead. Immediately after cutting, the samples were put in an infrared oven and held at a temperature of 400 °C for 20 min. The amount of diffusible hydrogen H_D was determined by thermal desorption mass spectroscopy (TDMS) technique with a mass spectrometer IPI ESD 100 based on the predetermined sample weight.

2.4 Cold crack testing and crack detection

Using the four-point-bend test device in Fig. 3 (left), the bending stress is set by a defined travel distance f and is measured

Table 5 Chemical composition of filler metal G3Si1 (wt.%) [15]

C	Si	Mn	P	S	Ni	Mo	Al	Ti + Zr
0.06–0.14	0.70–1.00	1.30–1.60	0.025	0.025	0.15	0.15	0.02	0.15

Table 6 Conditions of the cold crack test samples

Condition 1 (soaked)	Condition 2 (DP10)	Condition 3 (DP45)	Condition 4 (H ₂ O)	Condition 5 (oil)
Press hardening	Press hardening	Press hardening	Press hardening	Press hardening
Soaking	D _p ≈ 10 °C	D _p > 45 °C	Soaking	Soaking
GMA welding	GMA welding	GMA welding	GMA welding with water on surface	GMA welding with oil on surface

by an adjustable gauge. In Fig. 3 (right), the increasing extreme fiber stress with increasing bending path is shown. This was experimentally determined in a conventional tensile test machine measuring force and traverse, and calculating Young's modulus E and the extreme fiber stress σ_{EF} .

$$E = \frac{F_y \cdot l^3 \cdot a^2}{2 \cdot I \cdot l^2 \cdot f} \left(1 - \frac{4 \cdot a^2}{3 \cdot l^2} \right) \quad (1)$$

F_y force, I geometrical moment of inertia.

The empirically determined extreme fiber stress is compared to the theoretical stress, which can be described by the following equation:

$$\sigma_{EF} = \frac{12 \cdot E \cdot t \cdot f}{(3l^2 - 4a^2)} \quad (2)$$

where E is Young's modulus; t , Sheet thickness; f , deflection between the center of the sample and the outer supports; l , distance between the two outer supports; and a , distance between the inner and outer supports.

In the elastic state, the empirically determined and the theoretically calculated extreme fiber stress are in good agreement.

Pretests with un-welded samples of 22MnB5 showed even at high hydrogen content ($H_D > 0.6$ ppm) and high travel distances ($f > 12$ mm) no cold cracking during four-point-bend testing. This is presumably because there is no multiaxial stress state present in homogeneous samples, which is necessary for the initiation of HACC.

To prevent premature effusion of diffusible hydrogen after the press hardening and welding, the samples were stored in liquid nitrogen. Before the application of the bending stress, a thermoregulation to room temperature was ensured.

To evaluate the hydrogen-dependent cold-cracking behavior, the samples were given visual inspections during and after the four-point-bend test. Samples either exhibit *cold cracking* after a certain amount of time or there was *no cold cracking and the samples were taken out of the test after 24 h*. In order to obtain information about the time to failure, i.e., the time until the occurrence of cracking in the strained samples during the four-point-bend test, the acoustic emission measurement technique was used. For this purpose, a sensor was applied and attached during the whole testing time to the strained test sample. The acoustic emission was recorded and evaluated with a Locan-320 by Physical Acoustics Corp.

3 Results and discussion

3.1 Absorption of diffusible hydrogen

The austenitization of the 22MnB5+AS150 samples at different dew points, as well as GMA welding with various hydrogen-containing media on the sheet surface, result in the absorption of diffusible hydrogen into the material. The results of the hydrogen measurements by TDMS technique are shown in Fig. 4 as the distribution of diffusible hydrogen along the weld bead for all tested conditions. A slight increase

Fig. 4 Hydrogen distribution in the GMA bead-on-plate welds at different conditions (left). Average hydrogen content of the GMA bead-on-plate welds (right)

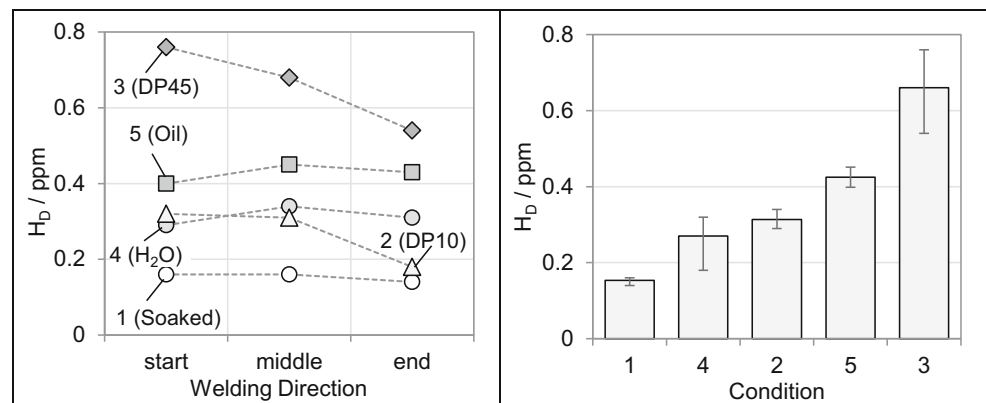
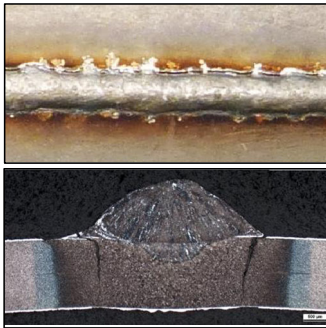


Fig. 5 Cold cracked bend test sample (left). Occurrence of cold cracking in all samples (o—no cold cracking; x—cold cracking) (right)



Condition	1 (Soaked)	4 (H ₂ O)	2 (DP10)	5 (Oil)	3 (DP45)
H _D					
f	0.15 ppm	0.27 ppm	0.31 ppm	0.43 ppm	0.61 ppm
0 mm	ooo	ooo	ooo	ooo	ooo
2 mm	ooo	ooo	ooo	ooo	ooo
4 mm	ooo	ooo	ooo	oxx	oox
5 mm	ooo	ooox	oox	xxx	ooxxx
6 mm	ooo	xxx	xxx	xxx	xxx
7 mm	oox	---	xxxxxx	xxx	xxx
8 mm	ooxxx	oxxxx	xxxxxx	xxx	xxx
9 mm	xxx	xxx	xxx	xxx	oxx
10 mm	xxx	xxx	xx	xxxxxx	xx

in hydrogen content was found to be present in the middle segments of the bead-on-plate welds.

For the samples welded with water on the surface (condition 4), a hydrogen content of about 0.3 ppm was measured. Similar hydrogen content was detected for the moderate dew point of 10 °C (condition 2), which is reflective of the conditions in industrially used furnaces for press hardening. The second highest hydrogen content of about 0.4 ppm was found in the samples which were welded with preservative oil (condition 5). The highest amount was detected at a dew point of 45 °C (condition 3) due to combustion gases in the furnace. A diffusible hydrogen content of about 0.7 ppm is quantified after GMA welding. In addition, some welded samples were soaked (condition 1). After 20 min at a temperature of 180 °C, a diffusible hydrogen content of about 0.15 ppm was determined.

The decrease of the hydrogen content at the end of the weld bead, when water was applied onto the surface before welding (condition 4), is probably due to water evaporation before the end of the welding process. For this reason, the mean value formed over the weld also is less than the oiled sample (condition 5), Fig. 4. A similar effect is observed with the high dew point (condition 3). Here, the hydrogen content reduces at the end of the weld due to the reheating that causes an effusion of hydrogen.

3.2 Cold-cracking behavior

If cracks occurred, they ran at the fusion line along the whole length of the GMA weld. To further describe the location of the cracking, a metallographic transverse section was prepared from each strained sample. Light optical microscopy showed that all cracks occurred right at the fusion line between the base metal and the weld metal independent of the sample conditions (1 to 5) or the hydrogen content, respectively. For a sample welded with oil on the surface, a close-up view and a transverse section are shown in Fig. 5 (left).

That the crack occurrence in the welded 22MnB5+AS150 samples at a distinct bending path primarily depends on the diffusible hydrogen is illustrated by the comparison of the number of torn or unimpaired bend samples (Fig. 5—right). With increasing hydrogen content in the samples, cold cracks occur at a smaller bending path or at a lower stress. This relationship is due to the reduction of material ductility by increased diffusible hydrogen [15]. It is notable that the oil-welded samples failed at a smaller bending path despite having a lower diffusible hydrogen content as the samples with the highest hydrogen content (condition 3).

The occurrence of cold cracking during the four-point-bend test can also be detected by looking at the sound emission recordings. In Fig. 6, two characteristic sound energy-time curves are schematically compared.

Fig. 6 Schematic curves of the cumulative sound energy for crack-free samples (left) as compared to samples with crack occurrence (right)

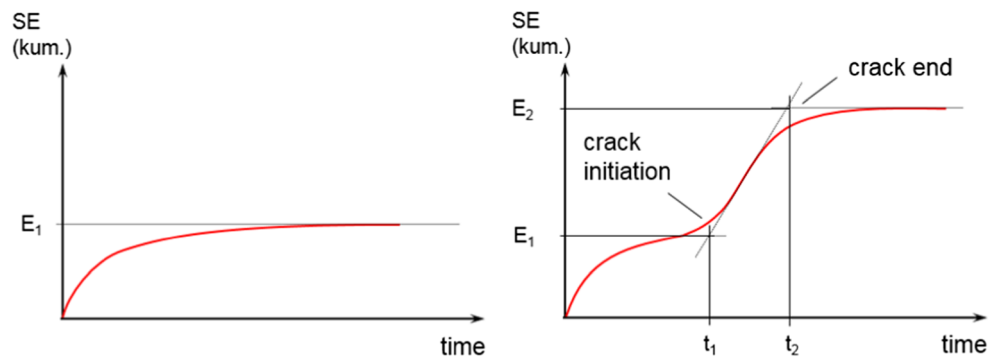
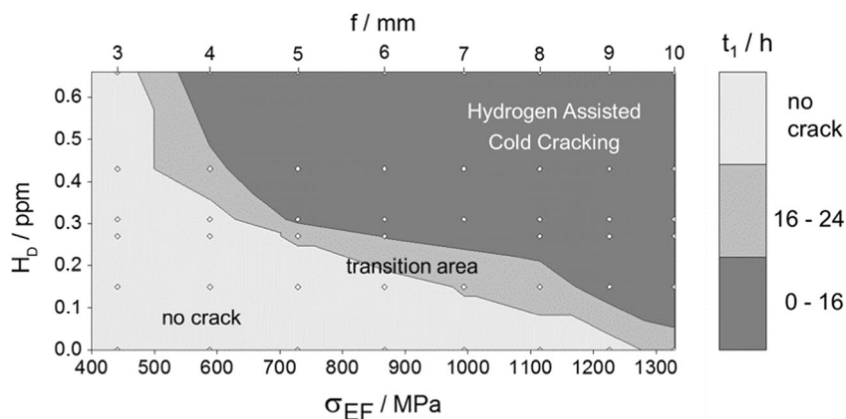


Fig. 7 Time to failure of GMA welded 22MnB5+AS150 samples in four-point-bend testing as a variation of hydrogen content and bending path (the *round marks* in the diagram are empirical tests corresponding to Fig. 5)



First, after applying the bending stress onto the sample, a rapid increase in the sound energy was recorded up to energy E_1 , which is related to the applied bending path, and which comes to a standstill after a time t_1 . This relationship is independent of the diffusible hydrogen content of the sample or a crack appearance at a later stage. Due to the very brittle and hard intermetallic phases in the Al-Si layer on the sheet surface of 22MnB5, it can be assumed this is the source of this sound energy.

While in the crack-free samples, no further change in the acoustic energy curve occurs over the test time, a sharp increase in the acoustic energy at time t_1 could be observed in samples, which cracked during bend testing. This increase in energy is accompanied by the crack initiation. It is therefore an adequate value for characterizing the time to failure of the bended test samples. After this relatively large increase in sound energy to E_2 , no further energy increase occurred. At time t_2 , the sample is considered to be completely cracked in the testing device. The duration of the damaging event can be determined from the time between the t_2 and t_1 .

In Fig. 7, the time to failure t_1 is reproduced in a contour plot as a variation of the hydrogen content and the maximum fiber stress applied to the sample.

Areas with different gray color represent different cold-cracking behavior. Samples in the light gray area did not crack during bend testing, whereas the darker gray color shows samples, which are more favorable to HACC and have a decreasing time to failure. Up to a maximum fiber stress of about 500 MPa ($f \approx 4$ mm) and the highest H_D content (condition 3) no cold cracking occurred in the samples. However, at a stress of about 1250 MPa ($f \approx 9$ mm) all samples failed, even those with an extremely low hydrogen content (condition 1). This stress value is slightly higher than the yield strength of the material.

A regression line was determined between all cracked and no cracked samples, based on which the detrimental effect of diffusible hydrogen in the welded samples of 22MnB5 can be characterized. With increasing hydrogen content, the time to failure decreases. In the same way, cold cracking occurs at smaller bending paths with increasing hydrogen content in the samples.

4 Summary

In summary, the following results can be obtained from this study:

- 22MnB5+AS150 absorbs diffusible hydrogen during austenitization in the furnace. The amount of hydrogen depends on the prevailing dew point in the furnace.
- Similarly, hydrogen-containing media on the sheet surface during GMA welding lead to a pickup of diffusible hydrogen into welded samples of 22MnB5+AS150.
- A heat treatment of 20 min at a temperature of 180 °C results in almost total hydrogen effusion from the material.
- The four-point-bend test is suitable for the provocation of HACC in 22MnB5.
- The acoustic emission technique is a good addition to the visual inspection for cold crack detection, allowing the determination of lifetime time to failure during four-point-bend testing.
- With increasing hydrogen content in the welded 22MnB5 samples, the maximum fiber stress required for the initiation of cold cracking in the four-point-bend test decreases; likewise, the time to failure decreases with an increasing hydrogen content in the samples.

References

1. Prange W, Schneider C (2001) Material steel - automobile light-weight initiatives of the international steel industry. *Stahl Eisen* 121(7):S. 23–29. (in German)
2. Merklinger V, Wielage B, Lampke T et al (2008) Development of low-temperature galvanizing and its application for corrosion protection of high-strength steels. *Mater Werkst* 39(12):S. 888–S. 891. doi:10.1002/mawe.200800395
3. Schulze G (2010) Die Metallurgie des Schweißens. Eisenwerkstoffe – Nichteisenmetallische Werkstoffe, Springer Heidelberg, 4. Auflage
4. Altan T (2007) Hot-stamping boron-alloyed steels for automotive parts. Part II: microstructure, material strength changes during hot stamping. *Stamping Journal* 1:S. 14–15
5. Georges C, Sturel T, Drillet P (2013) Absorption/desorption of diffusible hydrogen in aluminized boron steel. *ISIJ Int* 53(8):S. 1295–S. 1304
6. Hou W, Cretteur L, Kelley S (2009) Effect of gap on AHSS RSW weldability. SAE International, Warrendale
7. Jüttner S (2013) Material and joining developments in bodywork. In: OvGU-IWF, Mook. (Hrsg.) 14. Sommerkurs Werkstoffe und Fügen, Tagungsband, Universität Magdeburg, Magdeburg. (in German)
8. Böllinghaus T, Kannengießer T (2008) Cold cracking tests-overview. *IIW-Doc. IIW-1982-08*
9. Loidl M (2014) Entwicklung einer Prüfmethodik zur Charakterisierung höchstfester Karosseriestähle hinsichtlich des Risikos zur Wasserstoff induzierten Rissbildung. Universität Stuttgart. Institut für Materialprüfung, Werkstoffkunde und Festigkeitslehre Stuttgart, Dissertation. (in German)
10. Jüttner S, Zinke M, Schwedler O (2013) Untersuchung des Wasserstoffgefährdungspotentials warmumgeformter Bauteile aus hochfestem Stahl, Europäische Forschungsgesellschaft für Blechverarbeitung e.V. (EFB) Hannover. (in German)
11. Schwedler O, Zinke M, Jüttner S (2012) Properties of welded joints of press hardened body components, taking the hydrogen induced material degradation into account. In: Große Schweißtechnische Tagung, Tagungsband (in German)
12. Schwedler O, Holtschke N, Benziger T (2014) Studies on the cold cracking behavior of GMA welded 22MnB5+AS150 sheets using acoustic emission testing. In: OvGU-IWF, M. (Hrsg.) 15. Sommerkurs Werkstoffe und Fügen, Tagungsband. Universität Magdeburg, Magdeburg, (in German)
13. Alexandrov B, Theis K, Streitenberger M (2005) Cold cracking in weldments of steel S 690 QT. *Welding in the world* 49(5/6): S. 64–S. 73
14. Kutz KH, Theis K (1987) Schallemissionsmessungen an geschweißten Bauteilen aus H60-3. *Schweisstechnik* 37(4):S. 150–52, (in German)
15. DIN EN ISO 14341–2011. Welding consumables—wire electrodes and weld deposits for gas shielded metal arc welding of non alloy and fine grain steels—classification.